# ONE STEP BEYOND: FROM THE EXPERIMENTAL INVESTIGATION OF DISCHARGING METHODS TO NUMERICAL OPTIMIZATION POTENTIAL OF ELECTRET FILTER MEDIA

M. Kerner[1*], K. Schmidt[2], S. Schumacher[3], C. Asbach[3] and S. Antonyuk[1]
[1] Institute of Particle Process Engineering, Technische Universität Kaiserslautern, Gottlieb-Daimler-Straße 44, 67663 Kaiserslautern, Germany;
[2] IT for Engineering (it4e) GmbH, Morlauterer Straße 21, 67657 Kaiserslautern, Germany;
[3] Institute of Energy and Environmental Technology e.V. (IUTA), Bliersheimer Straße 58-60, 47229 Duisburg, Germany
*Corresponding author: maximilian.kerner@mv.uni-kl.de

## ABSTRACT

Electret filter media are commonly used in aerosol filtration to remove fine particles from gases. In addition to the mechanical deposition mechanisms, particles are deposited by electrostatic effects as the fibers are electrostatically charged. However, the particle deposition is reduced within operation, since already deposited particles alter the fiber charge and thus weaken the above-mentioned electrostatic effects. Standards mimic this ageing by discharging with isopropanol (IPA).

In this work discharged electret filter media were experimentally investigated applying different discharging methods (liquid IPA vs. IPA vapor), while the media are exposed to a sodium-chloride test aerosol with a bipolar equilibrium charge distribution. The test aerosol is therefore conducted through an aerosol neutralizer. The particle size distribution is measured upstream and downstream the electret filter media with a Scanning Mobility Particle Sizer obtaining the filtration efficiency. It could be shown that the air permeability or pore size are the main parameters influencing the discharge efficiency. For small pores, the discharge efficiency is reduced using liquid IPA, while for larger pores both discharging methods are applicable.

Moreover, simulations were performed for electrostatic charge optimization regarding the filtration efficiency using the in-house developed software DNSlab. A suitable 3D model of the fibrous structure is obtained by a mathematical algorithm, where charge is modeled on the fiber surfaces. The particle trajectories are calculated using the Euler-Lagrange approach considering the forces resulting from the calculated flow field through the 3D model and from the calculated electric field in the pore volume around the charged fiber surfaces. It could be shown that a homogeneous charge distribution within the filter depth is advantageous for the initial filtration efficiency. In contrast, a more pronounced charge in the filter middle delays charge decay and thus increases the lifetime, although a slightly lower initial filtration efficiency must be accepted.

## KEYWORDS

Direct Numerical Simulation, Discharging method, Electret, Optimization potential

## 1. INTRODUCTION

Electret filter media are commonly used in aerosol filtration to remove fine particles from gases. They provide a high initial particle removal efficiency combined with a low pressure drop as the fibers of the electret filter media are electrostatically charged. In addition to the mechanical deposition mechanisms (diffusion, impaction and interception), charged particles are deposited by the Coulomb effect and any (charged or uncharged) particles by dielectrophoresis [Wang2001].

The high initial particle deposition is reduced with increasing operating time, as already deposited particles attenuate the electrostatic effects mentioned above [Wang2001]. In the worst case, the electrostatic effects have vanished and the aged electret filter media become conventional mechanical filter media. With regard to the application, it is necessary that even the aged filter media achieve a minimum filtration efficiency. For this reason, standards mimic the ageing by discharging the electret filter media or the entire filter with IPA. The focus of this work is on the discharging methods with isopropanol prescribed in EN 779 (liquid IPA) and in ISO 16890-4 (IPA vapor).

It has been shown that the immersion in liquid IPA can lead to a structural change of the filter medium and thus to a different filtration efficiency compared to conditioning in IPA vapor. For example, an increasing thickness was observed for glass fiber medium after immersing and subsequent drying, which was explained by the dissolution of binders and the resulting loosening of the fibrous structure itself [Sun2009].

In [Myers2003] was also reported that the glass transition temperature of the fiber material changed after treatment with liquid IPA, which suggests an irreversible change in the structure of the polymer due to swelling in the solvent. Furthermore, a significant increase in flow resistance was observed for a filter medium with a nanofiber layer, which is due to a significant structural change in the nanofiber layer as a result of the liquid IPA treatment [Sun2009].

By comparing the resulting filtration efficiencies, it has also been observed that IPA vapor leads to a more efficient discharge of electret filters than the immersion in liquid IPA [Tronville2012]. This could be due to the fact that only a small discharge occurs when the polymer swells poorly in the solvent [Xiao2014]. However, this could not be confirmed when the Hansen solubility parameters for the polymers and IPA describing the swelling properties were compared [Schumacher2018]. Thus, the aim of this work is a detailed examination of parameters influencing the above mentioned discharging methods by deposition experiments using a submicron sodium-chloride test aerosol and different electret filter media.

In this and almost all other previous investigations the performance of existing electret filers and influencing factors were described. However, simulation setups allow a step towards filter optimization. Potentially optimizable electrostatic charge properties (e.g. spatial distribution on the fibers and the amount) regarding the filtration efficiency can be manipulated easily and in a time-optimized way with simulations. The aim of this work is therefore also to identify the optimization potential of electret filters using the previously validated simulation setup [Kerner2018, Kerner2020a, Kerner2020b].

## 3. EXPERIMENTS

The submicron sodium-chloride test aerosol is generated with a self-constructed collison nebulizer using particle-free pressurized air filtered by a HEPA-filter. After generation the test aerosol is conducted through a diffusion dryer and an aerosol neutralizer (TSI Model No. 3012A) to obtain a bipolar equilibrium charge distribution.

The particle size distribution is measured upstream and downstream the electret filter media samples with a Scanning Mobility Particle Sizer (SMPS, TSI Model No. 3934). On the upstream side is the particle size distribution in the range from 14 to 500 nm with a mode of 35 nm and an overall concentration of $10^6$ particles per $cm^3$. Based on the ratio of the downstream concentration to the upstream concentration of a particle size fraction the filtration efficiency for this size fraction is obtained.

Ten different electret filter media were investigated. The following table provides relevant information about them. The air permeability was obtained for a pressure drop of 200 Pa.

Table 1: Information on the electret filter media and the obtained air permeability

| Filter medium | Material | Manufacturing process | Charging method | Air permeability $L \cdot m^{-2} \cdot s^{-1}$ |
|---|---|---|---|---|
| 1 | Polypropylene | Unknown | Corona charged | 2527 ± 227 |
| 2 | - | Meltblown | - | 101 ± 3 |
| 3 | Polypropylene | Meltblown | Corona charged | 705 ± 13 |
| 4 | Polyamide nanofiber layer on a polyethylene + polypropylene supporting layer, | Spunbond (supporting layer) | Corona charged | 895 ± 177 |
| 5 | Polypropylene on a polyethylene-terephthalate supporting layer | Meltblown (supporting layer) | Corona-charged | 712 ± 44 |
| 6 | Polypropylene | Spunbond | - | 444 ± 56 |
| 7 | Polymer-Blend | - | Triboelectrically charged | 4473 ± 111 |
| 8 | Polymer-Blend | - | Triboelectrically charged | 4407 ± 222 |
| 9 | Polymer-Blend | - | Triboelectrically charged | 3105 ± 408 |
| 10 | Polymer-Blend | - | Triboelectrically charged | 1889 ± 121 |

The filtration efficiency was obtained before and after discharging the electret filter media samples according to EN 779 (5 min immersion in liquid IPA) and ISO 16890-4 (24 h conditioning in IPA vapor). Also the influence of the different treatment durations was investigated, immersing the media samples for 24 h in liquid IPA. Regarding the fibrous structure, no significant change was observed indicated by comparable air permeability after the discharging. Only for electret filter medium 4 the air permeability changed after liquid immersion revealing a structural change due to the liquid IPA treatment.

Electret filters are used to increase the particle deposition in the size range around 300 nm, as this is where the least influence of the mechanical deposition occurs known as MPPS (Most Penetrating Particle Size). Conversely, the filtration efficiency for a particle size of 300 nm can be used to determine whether a residual charge remains after the discharging. The corresponding values are shown in the following table 2, with the exception of electret filter medium 4. A representative comparison is not possible due to the structural change mentioned above.

Table 2: Filtration efficiency for a particle size of 300 nm depending on the filter medium and the discharging method

| Filter medium | 1 | 2 | 3 | 5 | 6 | 7 | 8 | 9 | 10 |
|---|---|---|---|---|---|---|---|---|---|
| Untreated | 0.77 | 1.00 | 0.97 | 0.97 | 0.85 | 0.93 | 0.90 | 0.97 | 0.99 |
| 5 min liq. IPA | 0.26 | 0.95 | 0.36 | 0.47 | 0.67 | 0.11 | 0.19 | 0.19 | 0.43 |
| 24 h liq. IPA | 0.13 | 0.87 | - | 0.35 | 0.55 | 0.09 | - | - | 0.35 |
| 24 h IPA vap. | 0.13 | 0.80 | - | 0.21 | 0.42 | 0.13 | - | - | 0.10 |

Immersion in liquid IPA results in a reduced discharge efficiency of the filter media with low air permeability (filter media 2, 5 and 6) compared to the filter media with high air permeability (filter media 1 and 7). When liquid IPA is used, the air must be displaced from the pores inside the fibrous structure during immersion. Low or high permeability can be represented as the presence of predominantly small or large pores. The passive process of immersion is then not sufficient to displace the air from the (small) pores of the filter media with low air permeability, so that the discharge is incomplete. In the case of IPA vapor, this phase boundary is not present when penetrating into the fibrous structure.

A further charge reduction by extending the immersion duration to 24 h is then possibly caused by molecular diffusion of the IPA molecules across the phase boundary. The extended immersion duration is advantageous for molecular diffusion as a statistically determined process and thus for mass transfer. As result, a comparable filtration efficiency was achieved for filter medium 1 after both 24 h treatments, which shows sufficient discharging of the filter media with high air permeability (filter media 1 and 7) by both liquid IPA and IPA vapor.

The explanation of the dependence on the air permeability is attributed to the wetting properties and molecular diffusion characteristics by simplified correlation with the pore size. With lower air permeability and correspondingly smaller pores, it should be noted that the particles also move closer to the fibers inside the fibrous structures. In addition, the electrostatic forces resulting from the electrostatic charge are mainly effective in the vicinity of the fibers. Consequently, a comparable residual charge could have a more pronounced effect on the particle deposition than in filter media with high air permeability.

However, numerical investigations (see chapter 4 for reference) with charged fibrous structures characterized by different porosities, fiber diameters and thicknesses, could exclude this. The additional effect of the electrostatic charge on the particle deposition remained constant.

## 4. 3D SIMULATIONS

A 3D model of the fibrous structure of the filter medium 1 is obtained by a mathematical algorithm generating a random distribution of cylinders (fibers) with 32 µm diameter perpendicular to the flow direction. New cylinders are added until the target porosity of 79 % and a thickness of 675 µm are reached using a hexaeder grid with an edge length of 1.5 µm for discretization. The size of the generated 3D model is 300 voxels in x-direction, 300 voxels in y-direction and 450 voxels in z-direction including an up- and downstream volume.

For calculation of the gas flow through the fibrous structure, the hexaeder grid is directly used for discretization of the following steady-state Navier-Stokes equations, which are solved with the finite differences method.

| | | | |
|---|---|---|---|
| $\mu\Delta\vec{V} - \rho(\vec{V}\cdot\nabla)\vec{V} = \nabla p$ | in $\Omega$ | (conservation of momentum) | [1] |
| $\nabla\cdot\vec{V} = 0$ | in $\Omega$ | (conservation of mass with constant density) | [2] |
| $\vec{V} = 0$ | on $\partial\Omega$ | (no-slip boundary condition) | [3] |

Here, $\vec{V}$ is the flow velocity, $p$ the pressure, $\mu$ the air viscosity and $\rho$ the air density. $\Omega$ is the flow domain of the 3D model and $\partial\Omega$ the fiber surface.

The charged areas of the fibers are modeled by random placing of spherical spots on the fiber surfaces to mimic triboelectrically charged filter media [Kerner2020a]. The charge inside the spots is described by the constant surface charge density $Q$, while the outer area is charged with -$Q$. Preliminary-investigations showed that the spot size should be within 50 % of the fiber diameter. To explain: with a fiber diameter of 32 µm, the spot size should be between 10 to 20 µm (average 15 µm). Otherwise the deviation in the filtration efficiency could already be caused by smaller spot sizes, which would not allow representative statements to be made.

For corona-charged filter, it seems appropriate to divide the entire structure, modeling one half as positively charged and the other half as negatively charged [Kerner2020a]. Obviously, a charge decrease in the filter depth is realistic because corona discharge is typically applied to the filter medium surface, resulting in a higher charge of the fibers near the surface compared to the fibers deeper inside the filter medium. Taking this consideration into account, various possible reductions from the surface to the center of the fibrous structure are realized when modeling the charge: from linear decrease to quadratic and exponential reduction.

For a defined surface charge density of 100 µC · m$^{-2}$, the electric field $\vec{E}$ in the pore volume around the charged areas is then calculated by explicit integration of the surface charges with following equation [4] of Stratton [Stratton1941]:

$$\vec{E}(\vec{X}) = \frac{1}{4 \cdot \pi \cdot \varepsilon_0} \cdot \int_{\partial\Omega} \frac{Q}{\| \vec{X} - \vec{S} \|^3} \cdot (\vec{X} - \vec{S})\, d\vec{S} \qquad [4]$$

In the equation $\vec{X}$ is the spatial position in Ω, $\vec{S}$ the surface integration variable and $\varepsilon_0$ the electric constant. To reduce the computation time equation [4] is only evaluated for $\vec{X}$ within less than 45 µm distance to fiber surface, while for distances more than 45 µm the electric field is set to zero. Previous investigations showed no deviation in the filtration efficiency when calculating the electric field in distance more than 45 µm.

With the resulting forces of the flow field and the electric field and additional diffusion, the particle movement through the fibrous structure is examined by calculation of the particle trajectories with the Euler-Lagrange approach [Schmidt2011]:

$$\vec{X}_P^{i+1} = \vec{X}_P^i + dt \cdot \vec{V}_P^i \qquad [5]$$

$$\vec{V}_P^{i+1} = \vec{V}_P^i + dt \cdot \frac{1}{m_P} \left( \gamma \cdot \left( \vec{V} - \vec{V}_P^i \right) + \vec{F}_C + \vec{F}_{Di} \right) + \mathcal{N}\left( 0, \sqrt{\frac{k_B \cdot T}{m_P}} \right) \qquad [6]$$

Here, $dt$ is the time step, $\vec{V}_P^i$ the particle velocity and $\vec{X}_P^i$ the particle position at the $i$-th time step. At the following $i+1$-th time step the particle velocity is set to $\vec{V}_P^{i+1}$ and the particle position to $\vec{X}_P^{i+1}$. The acceleration by the Coulomb force $\vec{F}_C$ and by dielectrophoresis $\vec{F}_{Di}$ are taken into account as effective electrostatic forces. The drag force is described by Stoke's law with the Cunningham correction $Cu$ in the particle-fluid friction coefficient $\gamma$ and $\mathcal{N}$ is the centered normal distribution with mean variation $\sqrt{\frac{k_B \cdot T}{m_P}}$ describing the Brownian particle motion.

$$\gamma = \frac{3 \cdot \pi \cdot \mu \cdot d_P}{Cu} \qquad [7]$$

$$\vec{F}_C = q \cdot \vec{E} \qquad [8]$$

$$\vec{F}_{Di} = \frac{\pi \cdot \varepsilon_0 \cdot d_P^3}{4} \cdot \left(\frac{\varepsilon_P - 1}{\varepsilon_P + 2}\right) \cdot \nabla \left|\vec{E}\right|^2 \qquad [9]$$

When the particle trajectories end on the fiber surfaces, the particles are considered as deposited and the filtration efficiency for a particle size fraction is obtained by the ratio of the number of deposited particles and the total particle number from that size fraction. Therefore, $10^6$ particles with diameters $d_P$ equally distributed in the range of 0.01 to 0.5 µm are tracked. The particle charge $q$ is generated according to the bipolar equilibirim charge distribution described by Wiedensohler [Wiedensohler 1988], while the relative dielectric constant of sodium chloride particles $\varepsilon_P$ is 5.9.

The obtained filtration efficiency depending on the different charge reductions from the surface to the center of the fibrous structure mentioned above is shown in the following figure 1.

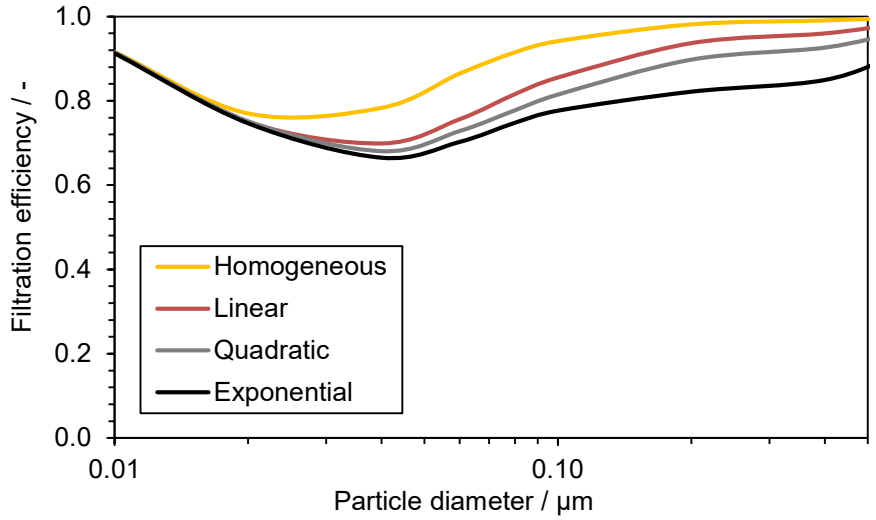


Figure 1: Calculated filtration efficiency depending on the decrease of charge intensity from the fibrous structure surface to the center.

As the electrostatic charge is reduced from the filter medium surface to the center, the particle deposition decreases. This is the more pronounced the more the charge decreases (exponential > quadratic > linear). The reason is the enlarged area in the fibrous structure center, where the electrostatic field is weak and therefore negligible with regard to the particle deposition due to dielectrophoresis and the Coulomb effect.

Regarding the corona charging of the filter medium, a homogeneous penetration of the fibrous structure (on both sides) with the charge carriers would be advantageous for a high initial particle deposition. In our previous work we found that the electrostatic field and thus the electrostatic charge alters with increasing particle deposition from the upstream to the downstream side of the fibrous structure [Kerner 2020b].

Conversely, a more pronounced charge in the fibrous structure center would lead to an extended operating time without significant decrease in filtration efficiency. Even if the electrostatic charges on the upstream side were altered due to deposited particles, there would still be enough charge left more downstream providing almost consistent particle deposition, although a slightly lower initial filtration efficiency must be accepted.

## 5. CONCLUSION

The influence of different discharging methods was experimentally investigated. It could be shown that the ISO 16890-4 provides a sufficient discharging procedure for all investigated electret filter media leading to a complete discharge while protecting the fibrous structure from structural changes.

Furthermore, it could be shown that the developed simulation setup is a helpful tool for the optimization of electret filter media with respect to the electrostatic charge. In a first step a suitable charge distribution on the fibrous structure was found which ensures high filtration efficiency even with increasing operating time.

## ACKNOWLEDGEMENT

The IGF project 19145 N is funded via the German Federation of Industrial Research Associations (AiF) within the program to support industrial collective research (IGF) by the German Federal Ministry for Economic Affairs (BMWi).

## REFERENCES

Kerner2018 Kerner et al. (2018), Numerical and experimental study of submicron aerosol deposition in electret microfiber nonwovens, Journal of Aerosol Science, Vol. 122, pp. 32-44

Kerner2020a Kerner et al. (2020), Evaluation of electrostatic properties of electret filters for aerosol deposition, Separation and Purification Technology, Vol. 239, 116548

Kerner2020b Kerner et al. (2020), Ageing of electret filter media due to deposition of submicron particles - Experimental and numerical investigations, Separation and Purification Technology, Vol. 251, 117299

Myers2003 Myers, D.L., Arnold, B.D. (2003), Electret Media For HVAC Filtration Applications, INJ Winter. Vol. 12, pp. 43–54

Schmidt2011 Schmidt, K. (2011), Dreidimensionale Modellierung von Filtrermediun und Simulation der Partikelabscheidung auf der Mirkoskala, Dissertation, Technische Universität Kaiserslautern

Schumacher2018 Schumacher, S., Jasit, R., Asbach, C. (2018), Einfluss von Entladungsmethode und Aerosolmaterial auf die Abscheideeffizienz von Elektretfiltern, Gefahrstoffe - Reinhaltung der Luft, Vol. 78, pp. 316-322

Stratton1941 Stratton, J. A. (1941), Electromagnetic Theory, McGraw-Hill

Sun2009 Sun, C (2009), Implication of Discharging Conditioning on Air Filter Media, International Technical Conference (INTC)

Tronville2012 Tronville, P., Rivers, R. (2012), Looking for the minimum efficiency of fibrous air filters during their service life. In: 11th World Filtration Congress Exhibition Proceedings

Wang2001 Wang, S.-C. (2001), Electrostatic forces in fibrous filters - a review, Powder Technology, Vol. 118, pp. 166-170

Wiedensohler1988 Wiedensohler, A. (1988), An Approximation of the Bipolar Charge Distribution for Particles in the Submicron Size Range, Journal of Aerosol Science, Vol. 19, pp. 387-389

Xiao2014 Xiao, H., Song, Y., Chen, G. (2014), Correlation between charge decay and solvent effect for melt-blown poly-propylene electret filter fabrics, Journal of Electrostatics, Vol. 72, pp. 311–314